

# Ambulatory measurement of shoulder and elbow kinematics through inertial and magnetic sensors

Andrea Giovanni Cutti · Andrea Giovanardi ·  
Laura Rocchi · Angelo Davalli · Rinaldo Sacchetti

Received: 21 April 2007 / Accepted: 24 November 2007 / Published online: 18 December 2007  
© International Federation for Medical and Biological Engineering 2007

**Abstract** Inertial and magnetic measurement systems (IMMSs) are a new generation of motion analysis systems which may diffuse the measurement of upper-limb kinematics to ambulatory settings. Based on the MT9B IMMS (Xsens Technologies, NL), we therefore developed a protocol that measures the scapulothoracic, humerothoracic and elbow 3D kinematics. To preliminarily evaluate the protocol, a 23-year-old subject performed six tasks involving shoulder and elbow single-joint-angle movements. Criteria for protocol validity were limited cross-talk with the other joint-angles during each task; scapulohumeral-rhythm close to literature results; and constant carrying-angle. To assess the accuracy of the MT9B when measuring the upper-limb kinematics through the protocol, we compared the MT9B estimations during the six tasks, plus other four, with the estimations of an optoelectronic system (the gold standard), in terms of RMS error, correlation coefficient ( $r$ ), and the amplitude ratio ( $m$ ). Results indicate that the criteria for protocol validity were met for all tasks. For the joint angles mainly involved in each movement, the MT9B estimations presented RMS errors  $<3.6^\circ$ ,  $r > 0.99$  and  $0.9 < m < 1.09$ . It appears therefore that (1) the protocol in combination with the MT9B is valid for, and (2) the MT9B in combination with the protocol is accurate when, measuring shoulder and elbow kinematics, during the tasks tested, in ambulatory settings.

**Keywords** Shoulder · Elbow · Kinematics · Inertial and magnetic sensors · Ambulatory measurement

## 1 Introduction

In the past 15 years, to assess elbow and shoulder 3D kinematics non-invasively, many different protocols have been developed, based on optoelectronic and electromagnetic measurement systems [1, 4, 30]. Although these protocols effectively describe pathologic upper limb biomechanics [12, 13, 16–18, 25, 27], they are uncommonly used in ambulatory settings, mostly due to limitations in the measurement systems. Optoelectronic and electromagnetic systems are costly, too complex, or too cumbersome to set up in small areas, such as a therapist's office, and have a limited field of view or of operation [3, 5].

One solution to overcome these drawbacks may be inertial and magnetic measurement systems (IMMSs), which are commercially available, low-cost, portable, and fully wearable motion analysis systems (InterSense, USA; Microstrain, USA; Xsens Technologies, NL). An IMMS consists of multiple sensing units (SUs), which are light-weight boxes. Each SU integrates an inertial measurement system, comprised of one 3D accelerometer and one 3D gyroscope, with a 3D magnetometer. The data supplied by the accelerometer, gyroscope, and magnetometer are combined through sensor-fusion algorithms [2, 21, 22] to measure the 3D orientation of the SU's system of reference (SoR)—defined based on the sensing axes of the inertial and magnetic sensors—with respect to a global, earth-based SoR. Given this 3D orientation, an IMMS has the potential to estimate joints kinematics when: (1) an SU is attached to each body segment of interest; (2) at least one

A. G. Cutti (✉) · A. Davalli · R. Sacchetti  
INAIL Prosthesis Center, Via Rabuina, 14,  
40054 Vigorso di Budrio (BO), Italy  
e-mail: agcutti@inail-starter.org

A. Giovanardi · L. Rocchi  
Department of Electronics, Computer Science and Systems,  
University of Bologna, Bologna, Italy

anatomical SoR is defined for each body segment; and (3) the orientation of the anatomical SoR is expressed in the SoR of the SU. Joints kinematics are finally obtained from the relative orientation of the anatomical SoRs, according to the International Society of Biomechanics (ISB) recommendations [30].

Only a few studies have investigated the use of IMMSs or simpler inertial measurement systems, to analyze the joint kinematics of the upper limb. These studies have mainly focused on determining the kinematics of the humerus [5], the humerothoracic [2] and the elbow [2, 14, 32]. To our knowledge, no study has used IMMSs to measure the scapulothoracic kinematics, which is a major issue in evaluating shoulder pathologies. In addition, estimates of humerus kinematics have been questionable for orthopaedic applications, with [5] reporting a mean RMS error of  $5.81^\circ$ . Other problems with current elbow kinematic models are that: (1) the model described in [32] is not based on a functional estimate of the elbow axes of rotation and is therefore prone to the kinematic coupling problem between elbow flexion–extension (FL-EX) and prono-supination (PR-SU) described in [7]; and (2) the model described in [14], although based on a functional estimate of the axes of rotation, constrains the carrying-angle to null, even though it is a constant, subject-specific angle [8, 28].

The purpose of this work was to develop a protocol to measure scapulothoracic, humerothoracic, and elbow kinematics in ambulatory settings, using the MT9B IMMS (hereinafter, “MT9B”; Xsens Technologies, NL). We then verified *in vivo* that: (1) the anatomical SoRs defined in the protocol allowed the actual kinematics of the upper limb to be measured, and (2) the MT9B was accurate when used to measure the upper limb kinematics through our protocol, during movements of clinical relevance.

## 2 Development of the protocol

### 2.1 The MT9B IMMS

The MT9B is an IMMS consisting of up to ten SUs connected by wire to a data-logger, usually worn on the belt. The data-logger is connected via Bluetooth to a laptop for data processing and data storage. Each SU is hosted in a small box, weights 38 g, and is  $39 \times 54 \times 28$  mm. The local SoR of the SU is aligned with the boundaries of the box with an error  $<3^\circ$  (Xsens Technical Manual; Fig. 1). The orientation of the each SU’s SoR with respect to an earth-based global SoR is provided as an output. For the present study the MT9B sampling frequency was fixed to 100 Hz.

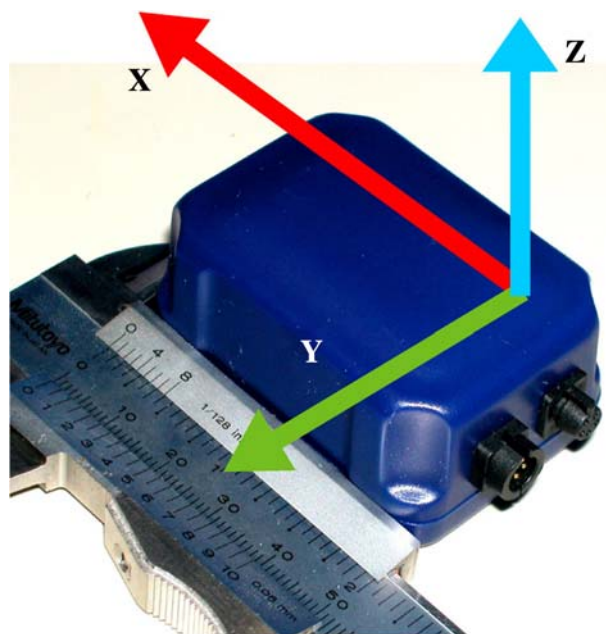


**Fig. 1** A MT9B’s SU with the sketch of its local SoR

### 2.2 Upper limb kinematic model

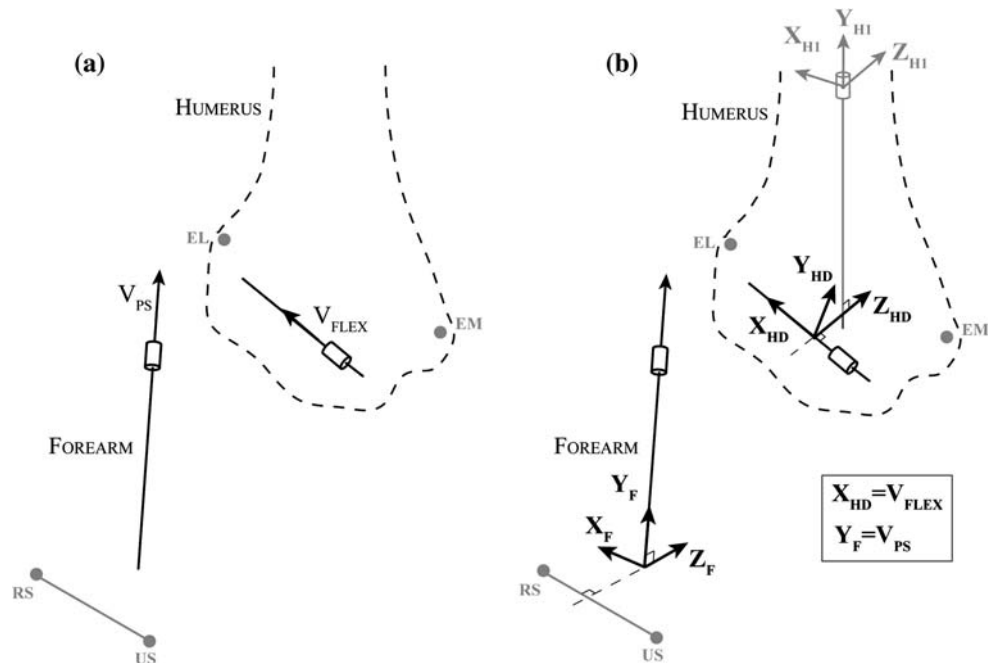
The upper limb kinematic model from which we developed the protocol was based on a set of assumptions involving the known functional and anatomical features of the shoulder and elbow.

#### 2.2.1 Body segments and kinematics description

In our kinematic model, the thorax, scapula, humerus, and forearm were assumed to be the rigid segments forming the upper limb. The orientations of the scapula and humerus were computed with respect to the thorax, while the orientation of the forearm was computed with respect to the humerus. Scapulothoracic kinematics was described by three independent angles: protraction–retraction (PR-RE), medio-lateral rotation (ME-LA) and anterior–posterior (AN-PO) tilting [30]. Humerothoracic kinematics was also described by three independent angles: flexion–extension (shFL-EX), ab-adduction (AB-AD) and internal–external rotation (IN-EX). The elbow was modeled, following [28], with two hinge joints with non-intersecting axes (Fig. 2a). Elbow kinematics was therefore described by two independent angles: flexion–extension (elFL-EX) and PR-SU—and a constant parameter, the carrying-angle. The carrying-angle measures the relative orientation of the axes of the hinges; it is subject-specific and not necessarily null [8, 28].

**Fig. 2** Kinematic model of the elbow, following [8, 28].

**a** Elbow hinge joints with non-intersecting axes of rotation: flexion–extension ( $V_{FLEX}$ ) and prono-supination ( $V_{PS}$ ); **b** anatomical SoRs for the distal humerus ( $X_{HD}Y_{HD}Z_{HD}$ ) and forearm ( $X_FY_FZ_F$ ).  $X_{H1}$ ,  $Y_{H1}$ , and  $Z_{H1}$  are the axes of the H1 anatomical SoR of the proximal humerus. The positions of the lateral epicondyle (EL), medial epicondyle (EM), radial styloid (RS), and ulnar styloid (US) are provided only as a guideline for interpretation: they were not involved in the computation.  $Z_F$  is drawn orthogonal to the line connecting RS and US to simply indicate that  $Z_F$  is defined as pointing posteriorly, away from the wrist



### 2.2.2 Outline of the anatomical systems of reference

To measure the scapulothoracic, humerothoracic, and elbow angles, we defined anatomical SoRs for the body segments of the upper limb. For the thorax and the scapula, the SoR axes were defined as close as possible to ISB recommendations [30].

For the humerus, we defined two sets of SoRs, (1) one descriptive of humerothoracic kinematics and related to the proximal humerus; and (2) the other descriptive of the elbow kinematics and related to the distal humerus. For the proximal humerus, we replicated both the H1 SoR described in [30], and the H2 SoR detailed in [30, 9]. For the distal humerus, the SoR was defined by applying the Denavit–Hartenberg method [24] at the elbow FL-EX hinge joint (Fig. 2b): (1) the  $X$  axis along the axis of rotation; (2) the  $Z$  axis orthogonal to the long axis of the proximal humerus and the  $X$  axis, pointing posteriorly; and (3) the  $Y$  axis orthogonal to the  $X$  and  $Z$  axes, pointing cranially.

The proximal humerus SoRs were not used to describe the elbow kinematics because approximating the elbow FL-EX axis with the H1 or H2 medio-lateral axis can lead to consistent errors when the elbow PR-SU angle is estimated [7].

For the forearm, the SoR was defined by applying the Denavit–Hartenberg method at the hand-effector of the elbow mechanism (Fig. 2b): (1) the  $Y$  axis along the axis of the elbow PR-SU hinge; (2) the  $Z$  axis pointing away from the wrist; and (3) the  $X$  axis orthogonal to the  $Y$  and  $Z$  axes.

The  $X$ ,  $Y$ , and  $Z$  labels assigned to the distal humerus and forearm SoRs differed from the standard Denavit–Hartenberg axis-labeling convention, to be consistent with ISB

recommendations ( $Z$  axis pointing backward, as preferred by the International Shoulder Group).

### 2.3 Protocol to assess upper-limb kinematics

The protocol to measure the scapulothoracic, humerothoracic and elbow kinematics of a subject using the MT9B consists of the following steps: (1) positioning the SUs on the subjects’ thorax, scapula, humerus, and forearm; (2) defining anatomical SoRs for the thorax, scapula, and proximal humerus, and expressing the SoRs orientation in the SU SoR of the corresponding segment; (3) defining anatomical SoRs for the distal humerus and the forearm, and expressing the SoRs orientation in the SU SoR of the corresponding segment; and (4) computing the joint angles. The protocol is described for the right arm only.

#### 2.3.1 Positioning the SUs

One SU is positioned on each body segment with double-sided tape, either over the skin or over elastic cuffs wrapped around the segments (Fig. 3). For the thorax, the SU is positioned over the flat portion of the sternum, with the  $Z$  axis of the SU pointing away from the body. For the scapula, the  $X$  axis of the SU is aligned with the cranial edge of the scapular spine, over the central third of the scapula. For the humerus the SU is positioned and oriented to minimize the soft tissue artefact: usually over the central third of the humerus, slightly posterior. For the forearm, the base of the SU is

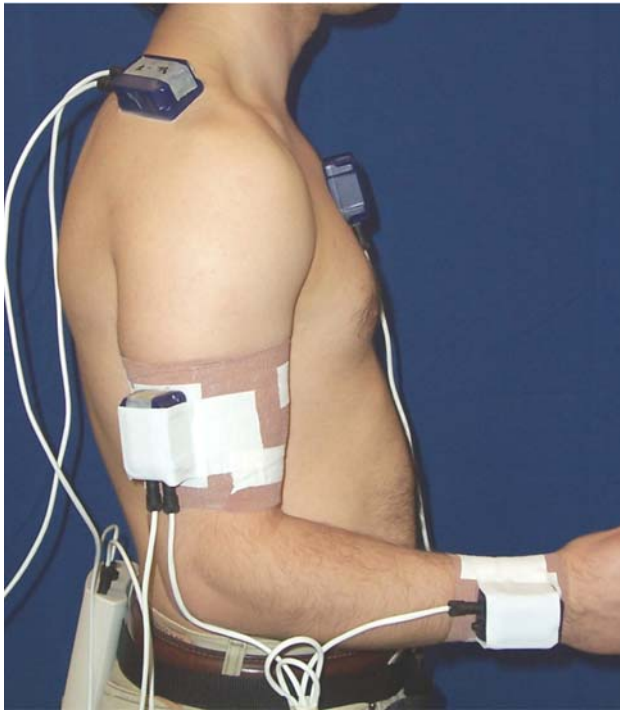


**Fig. 3** Positioning of the MT9B SUs on a subject

positioned over the distal, flat surface of radius and ulna, with the local Z axis pointing away from the wrist.

### 2.3.2 Defining the thorax, scapula, and proximal humerus anatomical SoRs

To define the anatomical SoRs of the thorax, scapula, and proximal humerus, and to express the orientation of these anatomical SoRs in the SU SoR of the corresponding segment, the orientation of the SUs' SoRs is measured during a static trial lasting 10 s. The subject is instructed to stand still, with his back straight and with both arms alongside the body, perpendicular to the ground.

The definitions of the anatomical SoRs (Table 1) are then applied. The anatomical SoRs of the thorax, scapula, and H1 have a constant orientation with respect to the SU SoR of the corresponding segment. In contrast, for H2, the orientation with respect to the SoR of the humerus SU is not constant, but is updated sample-by-sample during every task, based on the orientation of the long axis of the forearm [9].

### 2.3.3 Defining the distal humerus and forearm anatomical SoRs

To define the anatomical SoRs for the distal humerus and forearm (see Sect. 2.2.2) and to express the orientation of these anatomical SoRs in the SU SoR of the corresponding

**Table 1** Definition of the anatomical SoRs (right arm)

| Segment               | Axes definition   |
|-----------------------|---|
| Thorax (TH)           | $Y_{TH} = {}^{SU-TH}Z_G // {}^{SU-TH}Z_G \parallel$ : cranial<br>$X_{TH} = Y_{TH} \wedge -[0 \ 0 \ 1] // Y_{TH} \wedge -[0 \ 0 \ 1] \parallel$ : lateral<br>$Z_{TH} = X_{TH} \wedge Y_{TH} // X_{TH} \wedge Y_{TH} \parallel$ : posterior |
| Scapula (SC)          | $X_{SC} = [1 \ 0 \ 0]$ : lateral<br>$Z_{SC} = X_{SC} \wedge Z_G // X_{SC} \wedge Z_G \parallel$ : posterior<br>$Y_{SC} = Z_{SC} \wedge X_{SC} // Z_{SC} \wedge X_{SC} \parallel$ : cranial  |
| Proximal humerus (H1) | ${}^{SU-H}R_{H1} = {}^{SU-H}R_{TH}$   |
| Proximal humerus (H2) | $Y_{H2} = Y_{H1}$ : cranial<br>$X_{H2} = Y_{H2} \wedge {}^{SU-H}Y_F // Y_{H2} \wedge {}^{SU-H}Y_F \parallel$ : lateral<br>$Z_{H2} = X_{H2} \wedge Y_{H2} // X_{H2} \wedge Y_{H2} \parallel$ : posterior                                   |
| Distal humerus (HD)   | $X_{HD} = V_{FLEX} // V_{FLEX} \parallel$ : lateral<br>$Z_{HD} = X_{HD} \wedge Y_{H1} // X_{HD} \wedge Y_{H1} \parallel$ : posterior<br>$Y_{HD} = Z_{HD} \wedge X_{HD} // Z_{HD} \wedge X_{HD} \parallel$ : cranial                       |
| Forearm (F)           | $Y_F = V_{PS} // V_{PS} \parallel$ : cranial<br>$X_F = Y_F \wedge [0 \ 0 \ 1] // Y_F \wedge [0 \ 0 \ 1] \parallel$ : lateral<br>$Z_F = X_F \wedge Y_F // X_F \wedge Y_F \parallel$ : posterior  |

For each segment, all vectors are expressed in the SoR of the SU positioned on the segment. The Z axis of the global SoR ( $Z_G$ ) is assumed to be opposed to gravity.  $V_{FLEX}$  and  $V_{PS}$  are the directions of the flexion–extension and pronosupination axes of the elbow. Unlike the other anatomical SoRs, H2 orientation in the humerus SU SoR is updated sample-by-sample, based on the orientation of the long axis of the forearm [9].

$SU-TH$  SU on thorax,  $SU-H$  SU on humerus

segment, the direction of elbow FL-EX and PR-SU axes is estimated first. The orientation of the SUs over the humerus and forearm is measured during two tasks. In the first, the subject is instructed to flex-extend the elbow up to  $130^\circ$  for five times, keeping a constant PR-SU and the humerus alongside the body. In the second, the subject is instructed to fully pronosupinate the forearm, keeping the elbow flexed  $90^\circ$  and the humerus alongside the body. In the first task, the direction of the elbow FL-EX axis is estimated using the functional method described in [26, 29], and expressed in the SoR of the SU over the humerus. In the second task, the same method is applied to estimate the PR-SU axis, which is then expressed in the SoR of the SU over the forearm.

The distal humerus and forearm anatomical SoRs are then computed and expressed in the SUs' SoR using the equations reported in Table 1.

### 2.3.4 Computing the joint angles

During data acquisition for a task, the orientation of the anatomical SoRs is updated sample-by-sample based on

the orientation of the SUs' SoR. The humerothoracic, scapulothoracic, and elbow angles (see Sect. 2.2.1) are then obtained, sample-by-sample, by decomposing the relative orientation of the anatomical SoRs with the following sequences of Euler angles: scapulothoracic PR-RE, ME-LA rotation, and AN-PO tilting with the sequence  $YZ'X''$ ; humerothoracic shFL-EX, AB-AD, and IN-EX with the sequence  $XZ'Y''$  for almost sagittal tasks; humerothoracic AB-AD shFL-EX and IN-EX with the sequence  $ZX'Y''$  for almost frontal tasks; elbow eFL-EX, carrying angle and PR-SU with the sequence  $XZ'Y''$ .

### 3 Testing of the protocol

The protocol developed was tested in vivo in two experiments that were executed simultaneously. The first aimed to determine, preliminarily, whether the anatomical SoRs defined in the protocol allowed the actual kinematics of the upper limb to be measured. The second aimed to assess the errors due to the use of the MT9B instead of an optoelectronic system, in the measure of the upper-limb kinematics using the protocol, during movements of clinical relevance. In other words, the second aimed to assess the accuracy of the MT9B when used to measure the upper-limb kinematics through the protocol, during movements of clinical relevance.

#### 3.1 Subject description

A 23-year-old, right-handed male participated in the experiments after signing an informed consent. A physical examination excluded any pathology in the subject's upper limbs.

#### 3.2 Experiment 1: testing of the anatomical systems of reference

To conclude that the anatomical SoRs of the protocol allowed the actual humerothoracic, scapulothoracic and elbow kinematics to be measured, the following criteria needed to be met, (1) there was only minimal cross-talk between joint angles, as measured when the subject executed single-joint-angle movements; in other words, when a movement primarily involved one joint angle only, the range of motion (RoM) of the other angles of the same joint was minimal, (2) the scapulohumeral rhythm was close to literature results [15], and (3) there was minimal (ideally null) RoM of the carrying angle during elbow FL-EX and PR-SU movements.

#### 3.2.1 Set-up and procedure

The MT9B was used to measure the humerothoracic, scapulothoracic and elbow kinematics following the protocol described in Sect. 2.

The subject was instructed to repeat the following six single-joint-angle tasks, five times each, elbow FL-EX, and PR-SU, shoulder FL-EX, and IN-EX (this task required the subject to keep the humerus alongside the body with the elbow flexed 90° and in neutral pronation), shoulder-girdle elevation–depression, and PR-RE. In each repetition, the subject cyclically executed the movement five times.

#### 3.2.2 Data analysis

For the IN-EX task, H2 was used instead of H1 to compute humerothoracic angles since H2 correctly estimates the humerus axial rotation since it is free from soft tissue artefact errors [6].

Twenty-five movement cycles were obtained for each task. To evaluate whether the minimal cross-talk criterion was met, for each task the mean RoM of each joint angle was computed, over the 25 movement cycles. To evaluate the scapulohumeral-rhythm criterion, we computed the ratio between the RoM of the scapulohumeral ME-LA rotation and the RoM of the shFE-EX during the shoulder FL-EX task. To evaluate the carrying-angle criterion, we computed the RoM of the carrying-angle during the elbow FL-EX and PR-SU tasks.

#### 3.3 Experiment 2: testing of the MT9B protocol-dependent accuracy

The dynamic accuracy of the MT9B depends on the SUs' direction, velocity and amplitude of rotation [Xsens Technical Manual, 10, 22, 32].

Therefore, using both the MT9B and an optoelectronic system (Vicon 460, Oxford Metrics, UK) that was assumed as the gold standard, we measured the upper-limb kinematics of the subject, while he performed movements of clinical relevance.

#### 3.3.1 Set-up and procedure

The MT9B and the optoelectronic system were used simultaneously according to the protocol in Sect. 2, to measure the subject's scapulothoracic, humerothoracic and elbow kinematics. To apply the protocol with the optoelectronic system, each MT9B SU was replicated by a cluster of four markers, mounted on a rigid plate

(12 cm × 12 cm), glued on the SU itself; for the thorax, humerus and forearm we used plastic plates, 34 g of weight; to make the scapula’s cluster particularly light-weight (11 g), we used a plate made of two corrugated cardboards glued inside two superficial, rigid, and flat cardboards. A local SoR was assigned to each cluster, parallel to the SoR of the corresponding SU: the assignment was made possible through a hand-eye calibration procedure performed before the experimental session [19].

The subject performed the six single-joint-angle tasks of Experiment 1, plus four additional tasks: a shoulder IN-EX with the arm abducted 90°, a shoulder AB-AD in the frontal plane, a hand-to-nape task in the sagittal plane, and a hand-to-top-of-head task in the frontal plane. The subject repeated each task five times. In each repetition, he cyclically executed the movement five times. The subject performed all tasks at a comfortable, self-selected speed.

3.3.2 Data analysis

Joint-angles data measured by the MT9B and the optoelectronic system were compared by computing the RMS error, the correlation coefficient (*r*), and the angular coefficient of the regression line (*m*). Since a linear relation was expected between joint-angles data measured by the two systems, *m* was computed only for the data with *r* > 0.7.

To characterize the overall accuracy of the MT9B, we computed the median and quartile values of RMS, *r*, and *m*. Median and quartile values were computed since RMS, *r* and *m* do not have normal distributions.

To further characterize the accuracy of the MT9B from a clinical perspective, for each task joint angles were divided in two groups: main joint angles (MJA) and non-main joint angles (NMJA). The MJA were the angles mainly involved in the movement and are known to have a direct clinical relevance (Table 2). RMS, *r*, and *m* median and quartile values were computed separately for MJA and

NMJA. Box-and-whiskers plots with notches were then obtained.

4 Results

4.1 Results for Experiment 1

Table 3 reports the mean RoMs of the scapulothoracic, humerothoracic and elbow angles, for each of the tasks.

The anatomical SoRs of thorax and proximal humerus (H1 and H2) allowed to measure the humerothoracic kinematics in accordance with the minimal cross-talk criterion. In particular, the correct identification of the humerothoracic FL-EX axis of rotation was supported by the very limited AB-AD (9° ± 1.9°) registered for the pure shoulder FL-EX task executed in the sagittal plane. Similarly, the correct identification of the IN-EX axis of rotation of the humerus was supported by the extremely limited shFL-EX and AB-AD (*worst-case* RoMs: 6° for shFL-EX; 2.6° for AB-AD) registered for the humerothoracic IN-EX task. As a consequence, it followed the correct identification of the humerothoracic AB-AD axis of rotation, which is, by definition, orthogonal to the FL-EX and IN-EX axes.

The anatomical SoRs of thorax and scapula allowed measuring the scapulothoracic kinematics in accordance with the minimal cross-talk criterion. In particular, during the shoulder-girdle elevation-depression task, the RoM measured for the scapulothoracic ME-LA rotation was more than three times the RoM measured for the scapulothoracic PR-RE and AN-PO, thus supporting the correct identification of the scapulothoracic ME-LA axis of rotation. Similar considerations apply to the shoulder-girdle PR-RE task: the RoM measured for the scapulothoracic PR-RE was from two to three times bigger than the scapulothoracic ME-LA rotation and AN-PO tilting, thus supporting the correct identification of the scapulothoracic PR-RE axis.

**Table 2** Main joint angles (MJA) and non-main joint angles (NMJA) considered in each task

White boxes MJA; gray boxes NMJA

IN-EX 1 IN-EX task executed with the humerus alongside the body, IN-EX 2 IN-EX task executed with the humerus abducted 90°, EL-DE elevation–depression, PR-RE protraction–retraction

| TASKS \ JOINTS        | ELBOW |    |       | HUMEROTHORACIC |       |       | SCAPULOTHORACIC |       |       |
|-----------------------|-------|----|-------|----------------|-------|-------|-----------------|-------|-------|
|                       | FL-EX | CA | PR-SU | FL-EX          | AB-AD | IN-EX | PR-RE           | ME-LA | AN-PO |
| Elbow FL-EX           |       |    |       |                |       |       |                 |       |       |
| Elbow PR-SU           |       |    |       |                |       |       |                 |       |       |
| Shoulder FL-EX        |       |    |       |                |       |       |                 |       |       |
| Shoulder AB-AD        |       |    |       |                |       |       |                 |       |       |
| Shoulder IN-EX 1      |       |    |       |                |       |       |                 |       |       |
| Shoulder IN-EX 2      |       |    |       |                |       |       |                 |       |       |
| Hand-to-nape          |       |    |       |                |       |       |                 |       |       |
| Hand-to-top-of-head   |       |    |       |                |       |       |                 |       |       |
| Shoulder-girdle EL-DE |       |    |       |                |       |       |                 |       |       |
| Shoulder-girdle PR-RE |       |    |       |                |       |       |                 |       |       |

**Table 3** Mean RoM ( $\pm 1$  SD) for the single-joint-angle tasks tested in Experiment 1

| TASK       | ELBOW          |                 |               | HUMEROTHORACIC  |             |                | SCAPULOTHORACIC |                |                |
|------------|----------------|-----------------|---------------|-----------------|-------------|----------------|-----------------|----------------|----------------|
|            | FL-EX          | PR-SU           | Carrying ang. | FL-EX           | AB-AD       | IN-EX          | PR-RE           | ME-LA          | AN-PO          |
| El. FL-EX  | 95.1 $\pm$ 4.8 | 5.5 $\pm$ 2.6   | 3.7 $\pm$ 0.7 |                 |             |                |                 |                |                |
| El. PR-SU  | 3.1 $\pm$ 1.3  | 114.2 $\pm$ 3.8 | 2.6 $\pm$ 0.7 |                 |             |                |                 |                |                |
| Sho. FL-EX |                |                 |               | 110.2 $\pm$ 3.1 | 9 $\pm$ 1.9 | 11.0 $\pm$ 3.6 | 18.5 $\pm$ 2.5  | 27.7 $\pm$ 2.4 | 9.1 $\pm$ 1.3  |
| Sho. IN-EX |                |                 |               |                 |             |                | 3.7 $\pm$ 1.4   | 1.7 $\pm$ 0.5  | 57.9 $\pm$ 5.3 |
| Gir. EL-DE |                |                 |               |                 |             |                |                 |                |                |
| Gir. PR-RE |                |                 |               |                 |             |                |                 |                |                |

All measures in degrees

El. elbow, Sho. shoulder, Gir. shoulder-girdle, EL-DE elevation–depression, PR-RE protraction-retraction

The correct identification of the anatomical SoR for thorax, scapula and proximal humerus was also confirmed by the results for the scapulohumeral-rhythm (Fig. 4). During shoulder FL-EX, the scapula ME-LA rotation remained almost steady until 40°. Then, on average, 28° of ME-LA rotation followed about 70° of humerothoracic FL-EX, with a 2.5:1 ratio which is close to expectations [15, 20].

The anatomical SoRs of the distal humerus and forearm allowed measuring the elbow kinematics in accordance with the minimal cross-talk and carrying angle criteria. In particular, the correct identification of the elbow axes of rotation was supported by the very limited PR-SU (5.5°  $\pm$  2.6°) during the elbow FL-EX task, and by the very limited FL-EX (3.1°  $\pm$  1.3°) during the PR-SU task. In addition, the RoM of the carrying-angle remained very close to zero, with only 3.7°  $\pm$  0.7° for the elFL-EX task and 2.6°  $\pm$  0.7° for the PR-SU task.

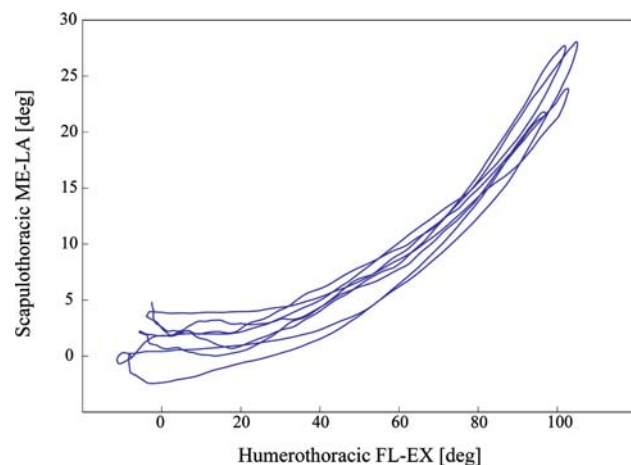


**Fig. 4** Scapulohumeral-rhythm measured during a shoulder FL-EX task performed in the sagittal plane. The repetitions of the movement performed by the subject during the task are reported

#### 4.2 Results for Experiment 2

Each joint angle measured by the MT9B was also measured by the optoelectronic system (Fig. 5), resulting in 450 pairs of data being compared. After excluding 24 of them due to recording problems, the RMS error,  $r$  and  $m$  for each of the remaining 426 pairs were computed.

Results for RMS,  $r$  and  $m$  demonstrated the considerable accuracy of the MT9B system, as well as its ability in generating angle data highly correlated and with magnitude close to the optoelectronic gold standard. For 97% of data pairs the RMS ranged between 0.2° and 3.2°; 90.4% had  $r$  above 0.86, and for 88%,  $m$  ranged between 0.79 and 1.15 (number of samples for  $m$ : 419).

Figure 6 reports the results for the RMS error,  $r$  and  $m$  after differentiating angle data in MJA and NMJA. The MJA data (164 samples) from the MT9B were found more correlated and closer in magnitude to the gold standard with respect to NMJA data (262 samples), with statistically significant differences for  $r$  and  $m$  ( $p < 0.05$ )—notches completely non-overlapping. More specifically, in 100% of MJA pairs  $r$  was  $>0.94$  (87%  $> 0.99$ ) and  $m$  ranged between 0.90 and 1.09 (89% were between 0.94 and 1.07). No statistically significant differences were found for RMS between MJA and NMJA.

In seeking an explanation for why the MT9B computed the kinematics of the MJA more accurately than it did for NMJA, we analyzed the differences in their RoM and mean velocity (Fig. 7). For each joint angle, the mean velocity was computed as the mean of the absolute value of the joint-angle first derivative. As reported in Fig. 7, MJA were generally characterized by higher mean velocities and RoMs, compared to NMJA. Given the different results obtained for  $r$  and  $m$ , it may be concluded that for MJA the positive influence of the higher RoM [22, 32] compensated for the negative influence of the higher mean velocity [10]. For NMJA, in contrast, the more limited RoM—which was reported as a factor negatively influencing the IMMS performances [22, 32]—could not be compensated for by any positive factor. This conclusion appears to be supported by

**Fig. 5** Joint angles measured by MT9B (*solid line*) and optoelectronic system (*dashed line*) for an elbow FL-EX task. MT9B estimates of elbow kinematics were very close to the optoelectronic system estimates in terms of RMS error, correlation ( $r$ ) and magnitude ( $m$ ). The extremely small RoM for the carrying-angle indicates the good estimation of the elbow FL-EX axis

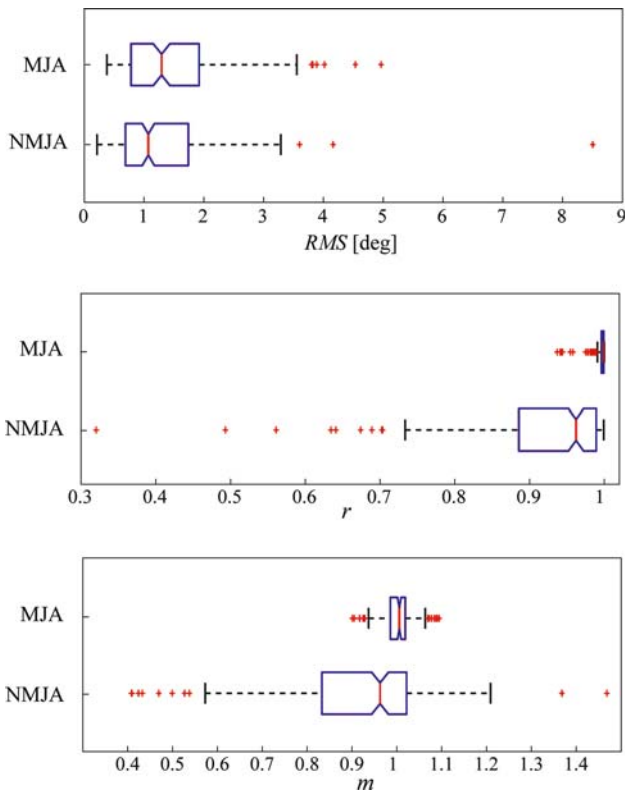
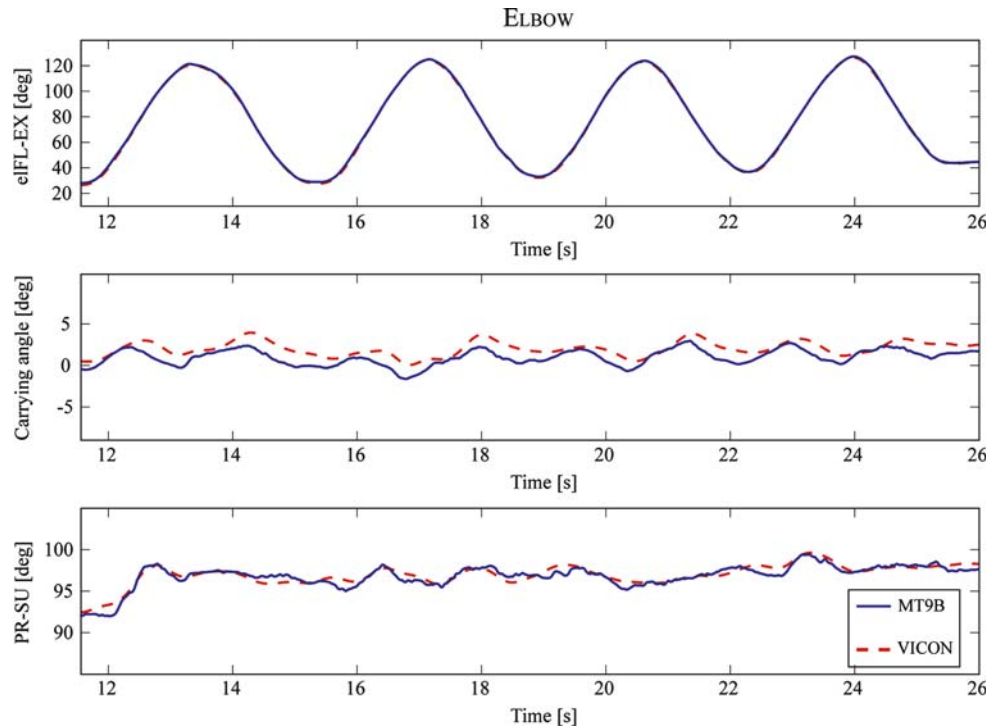


**Fig. 6** Box-and-whisker plots with notches for RMS,  $r$  and  $m$ , after differentiating angle data in MJA and NMJA

the outliers in the NMJA groups for  $r$  and  $m$ , which were characterized by extremely small RoMs (average RoM = 6°).

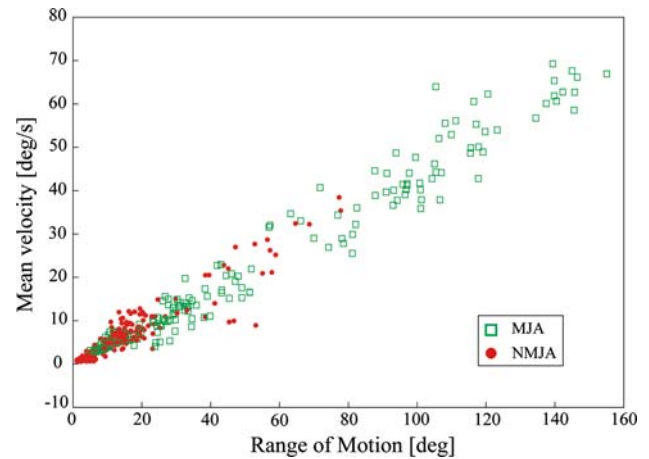


**Fig. 7** Relation between mean velocity and RoM featuring the data of MJA and NMJA. For each joint angle, the mean velocity was computed as the mean of the absolute value of the joint-angle first derivative. Each *square* (MJA) or *dot* (NMJA) represents a single angle data: 164 squares and 262 dots are reported

### 5 Discussion and conclusions

IMMSs are commercially available, low-cost, portable, and fully wearable, and are therefore good candidates to be used in ambulatory settings to measure shoulder and elbow kinematics, through the protocol presented in this paper.

The protocol requires a MT9B SU to be simply attached on the thorax, scapula, humerus, and forearm and defines anatomical SoRs for these body segments through one static acquisition and the functional estimate of the



elbow axes of rotation. The protocol takes <10 min to complete, and it does not require any additional device other than the MT9B system itself. In addition, the MT9B provides as an output the orientation of the SUs SoR; the computation of joint angles, therefore, does not require the development of sensor-fusion algorithms [5, 14, 32] or data conditioning through biomechanical models [14, 32].

The protocol does not take into account any movement of the clavicle. Clavicle tracking was excluded due to the physical dimensions of the SU, which prevented it from being securely and comfortably attached over the clavicle.

The SUs are attached to the skin and are not fixed to the bone resulting in upper limb kinematics possibly being affected by soft tissue artefacts. Regarding the scapula SU, however, Karduna et al. [11] showed that an electromagnetic sensor positioned on the skin over the acromion can measure scapula kinematics up to 120° of humeral elevation, with an accuracy suitable for clinical applications [13]. In addition, results from Experiment 1 suggest the possibility to track the scapula motion with the MT9B positioned over the scapula as described in the protocol. In particular, the 2.5:1 ratio measured for the scapulohumeral-rhythm was close to previous findings. Regarding the humerus SU, the use of H2 in the humerothoracic IN-EX task circumvented the soft-tissue artefact problem [6]. During the other tasks, the measure of IN-EX should be evaluated with caution. Future efforts will be made to integrate in the protocol the compensation techniques developed by these authors [9] and by Schmidt et al. [23]. As a general indication regarding soft tissue artefact, intra-subject comparisons, e.g. “affected side versus sound side”, appear less critical, since they allow, de facto, to neglect larger inter-individual differences related to soft tissue consistency (e.g. muscle mass, fat mass, skin elasticity).

Results from Experiment 1, which tested just one subject, provided a promising preliminary assessment of the protocol validity: all the criteria defined in Experiment 1 were met, supporting the conclusion that the anatomical SoRs defined in the protocol allow the actual upper limb kinematics to be measured. The subject involved in Experiment 1 performs a regular physical activity and has an excellent muscle tone and skin elasticity, with a body mass index equal to 18.6 (normal weight). As discussed in the previous paragraph, this might have affected the magnitude of the soft tissue artefact error. In particular, the subject’s characteristics might have positively influenced the scapula tracking. On the other end, given the good results for the carrying angle, we can conclude that the variation of the biceps belly during elbow FL-EX and PR-SU did not substantially influence the estimation of the

elbow axes of rotation. We are now testing many more subjects of different ages and body mass, suffering from shoulder and elbow orthopedic pathologies, to further assess the clinical validity of the protocol. It is worth noting that Experiment 1 was very simple and fast to perform, suggesting that it may be a convenient tool for use in ambulatory settings, to verify that the protocol has been correctly executed.

Results from Experiment 1 justified the execution of Experiment 2. Results from Experiment 2 confirmed that the accuracy of the MT9B is adequate for clinical applications, when used to measure the upper-limb kinematics with the protocol developed, during the tasks selected. Results from Experiment 2 were obtained comparing the upper-limb kinematics measured by the MT9B and by the optoelectronic system using the same protocol. This allowed to exclude differences in the measurements of the two systems due to the use of different anatomical SoRs, such as the differences that might have followed applying the protocol presented here with the MT9B, and the ISB standard [30] with the optoelectronic system. Moreover, the clusters of markers were glued on the SUs to ensure that the *same* soft-tissue artefact affected both tracking devices, thus making the artefact negligible in the comparison between the kinematics read by the two systems. Consequently, the differences in the upper-limb kinematics could be directly related to the intrinsic accuracy of the MT9B and to how the MT9B instrumental errors propagate through the protocol (e.g. in the estimation of the elbow functional axes of rotation); that is, the differences could be traced back to the accuracy of the MT9B when measuring the upper-limb kinematics through the protocol. To the authors’ knowledge, no studies have previously analyzed the accuracy of the MT9B in combination with a specific protocol, and in relation to RoM and velocity. Results for the MT9B accuracy were obtained for a young healthy subject performing movements at a self-selected speed. For patients with pathologies at the shoulder or elbow, such as rotator-cuff tears, shoulder instability or requiring a joint prosthesis, slower movements are expected for similar RoMs, which should lead to even better MT9B accuracy.

In a future perspective, the integration of the protocol presented here with (1) the measure of wrist, elbow and shoulder position presented in [31, 32], and (2) the functional indexes presented in [5], could result in an effective and comprehensive tool for the clinical assessment of patients with shoulder disorders.

**Acknowledgments** This work was supported by Regione Emilia-Romagna, in the framework of the Starter Project, PRRITT—Misura 3.4 Azione A.

## References

1. Anglin C, Wyss UP (2000) Review of arm motion analyses. *Proc Inst Mech Eng [H]* 214:541–555
2. Bachmann ER, McGhee RB, Yun X, Zyda MJ (2001) Inertial and magnetic posture tracking for inserting humans into networked virtual environment. In: *Proceedings of the ACM symp virtual reality software and technology*, pp 9–16
3. Best R, Begg R (2006) Overview of motion analysis and gait feature. In: Begg R, Palaniswami M (eds) *Computational intelligence for movement sciences*. IGP pp 1–69, Hershey, Pennsylvania, USA
4. Biryukova EV, Roby-Brami A, Frolov AA, Mokhtari M (2000) Kinematics of human arm reconstructed from spatial tracking system recordings. *J Biomech* 33:985–995
5. Coley B, Jolles BM, Farron A, Bourgeois A, Nussbaumer F, Pichonnaz C, Aminian K (2006) Outcome evaluation in shoulder surgery using 3D kinematics sensors. *Gait Posture*. doi:10.1016/j.gaitpost.2006.06.016
6. Cutti AG, Paolini G, Troncosi M, Cappello A, Davalli A (2005) Soft tissue artefact assessment in humeral axial rotation. *Gait Posture* 21:341–349
7. Cutti AG, Garofalo P, Davalli A (2006) How accurate is the estimation of elbow kinematics using ISB recommended joint coordinate systems? *Gait Posture* 24:S36–S37
8. Cutti AG, Raggi M, Davalli A, Cappello A (2006) Definition of two reference elbow models from cadaver data. *Gait Posture* 24:S224–S225
9. Cutti AG, Cappello A, Davalli A (2006) In-vivo validation of a new technique for soft tissue artefact compensation at the upper-arm: preliminary results. *Clin Biomech (Bristol, Avon)* 21:S13–S19
10. Cutti AG, Giovanardi A, Rocchi L, Davalli A (2006) A simple test to assess the static and dynamic accuracy of an inertial sensors system for human movement analysis. In: *Proceedings of the 28th IEEE EMBS annual international conference SaEP61*, pp 5912–5915
11. Karduna AR, McClure PW, Michener LA, Sennett B (2001) Dynamic measurements of three-dimensional scapular kinematics: a validation study. *J Biomech Eng* 123:184–190
12. Lockard M (2006) Clinical biomechanics of the elbow. *J Hand Ther* 19:72–80
13. Ludewig PM, Cook TM (2000) Alterations in shoulder kinematics and associated muscle activity in people with symptoms of shoulder impingement. *Phys Ther* 80:276–291
14. Luinge HJ, Veltink PH, Baten CT (2007) Ambulatory measurement of arm orientation. *J Biomech* 40:78–85
15. McClure PW, Michener LA, Sennett BJ, Karduna AR (2001) Direct 3-dimensional measurement of scapular kinematics during dynamic movements in vivo. *J Shoulder Elbow Surg* 10:269–277
16. McClure PW, Michener LA, Karduna AR (2006) Shoulder function and 3-dimensional scapular kinematics in people with and without shoulder impingement syndrome. *Phys Ther* 86:1075–1090
17. Mell AG, LaScalza S, Guffey P, Ray J, Maciejewski M, Carpenter JE, Hughes RE (2005) Effect of rotator cuff pathology on shoulder rhythm. *J Shoulder Elbow Surg* 14:58S–64S
18. Meskers CG, Koppe PA, Konijnenbelt MH, Veeger DH, Janssen TW (2005) Kinematic alterations in the ipsilateral shoulder of patients with hemiplegia due to stroke. *Am J Phys Med Rehabil* 84:97–105
19. Park FC, Martin BJ (1994) Robot sensor calibration: solving  $AX = XB$  on the Euclidean group. *IEEE Trans Rob Autom* 10(5):717–721
20. Pascoal AG, van der Helm FF, Pezarat CP, Carita I (2000) Effects of different arm external loads on the scapulo-humeral rhythm. *Clin Biomech (Bristol, Avon)* 15(Suppl 1):S21–S24
21. Roetenberg D (2006) Inertial and magnetic sensing of human motion. Ph.D. thesis, Twente University
22. Sabatini AM (2006) Inertial sensing in biomechanics: a survey of computational techniques bridging motion analysis and personal navigation. In: Begg R, Palaniswami M (eds) *Computational intelligence for movement sciences*. IGP pp 70–100, Hershey, Pennsylvania, USA
23. Schmidt R, Disselhorst-Klug C, Silny J, Rau G (1999) A marker-based measurement procedure for unconstrained wrist and elbow motions. *J Biomech* 32:615–621
24. Sciavicco L, Siciliano B (2000) *Modelling and control of robot manipulators*. Springer-Verlag, New York
25. Steenbrink F, de Groot JH, Veeger HE, Meskers CG, van de Sande MA, Rozing PM (2006) Pathological muscle activation patterns in patients with massive rotator cuff tears, with and without subacromial anaesthetics. *Man Ther* 11:231–237
26. Stokdijk M, Biegstraaten M, Ormel W, de Boer YA, Veeger HE, Rozing PM (2000) Determining the optimal flexion-extension axis of the elbow in vivo—a study of interobserver and intraobserver reliability. *J Biomech* 33:1139–1145
27. Stokdijk M, Nagels J, Garling EH, Rozing PM (2003) The kinematic elbow axis as a parameter to evaluate total elbow replacement: a cadaver study of the iBP elbow system. *J Shoulder Elbow Surg* 12:63–68
28. Veeger HE, Yu B, An KN, Rozendal RH (1997) Parameters for modelling the upper extremity. *J Biomech* 30:647–652
29. Woltring HJ (1990) Data processing and error analysis. In: Cappozzo A, Berme N (eds) *Biomechanics of human movement*. Bertec Corporation, pp 203–237, Worthington, Ohio, USA
30. Wu G, van der Helm FC, Veeger HEJ, Makhsous M, van Roy P, Anglin C, Nagels J, Karduna A, McQuade K, Wang X, Werner FW, Buchholz B (2005) ISB recommendation on definitions of joint coordinate systems of various joints for the reporting of human joint motion—part II: shoulder, elbow, wrist and hand. *J Biomech* 38:981–992
31. Zhou H, Hu H, Tao Y (2006) Inertial measurements of upper limb motion. *Med Biol Eng Comput* 44:479–87
32. Zhou H, Stone T, Hu H, Harris N (2007) Use of multiple wearable inertial sensors in upper-limb motion tracking. *Med Eng Phys*. doi:10.1016/j.medengphy.2006.11.010